

UGC
Minor Research Project Report

Submitted by

Neeta B Srivastava

Dept of Physics

Ramniranjan Jhunjhunwala College, Ghatkopar
Mumbai (2012-2014)

Objective: To investigate the mechanism of transport and the nature of charge carriers in conducting carbon nanotubes.

Introduction:

Carbon nanomaterials are among the most exciting new materials to have been discovered in the past 30 years. Their remarkable properties have attracted intense interest from the scientific community, as well as from industry. With the emergence of nano science and technology, research has been initiated to exploit the unusual and unique properties of carbon nanomaterials (CNMs). CNMs may exist in several forms, such as, single-walled carbon nanotubes (SWCNTs), multi-walled carbon nanotubes (MWCNTs), carbon beads, carbon fibres and nanoporous carbon. CNMs have been studied widely for potential applications in catalyst supports, optical devices, quantum computer, and biochips. However, their conduction potential has not been studied extensively. CNMs are engineered materials targeted to exhibit unique surface morphologies; hence, they may prove to be good sorbents [1] too.

At the nanometric scale the properties of the materials are different than the three-dimensional bulk forms due to difference in bond strength and short-and long-range bond order. Efforts are made to understand the correlation between the structure and properties of the materials with nanoscale diameter and with lengths varying in the micron range. Currently Nanofibers are used in industry for insulation and reinforcement of composites. Nanomaterials have been developed for use in lightweight composite materials for space and aircraft industry. Commercial fibres are of typically of order $7\mu\text{m}$ that have strength and bulk modulus 1.5 and 200Gpa. The single and multi-walled nanotubes with diameter in the nm and

length in the μm range have superior mechanical properties and have received wide attention recently. The development with nano-materials of a range of new devices in areas like electronics, photovoltaics, sensing, photonics and thermoelectric power is being actively pursued.

Though many other materials besides carbon have been produced in nanometre size but carbon nanomaterials have shown potential applications.

materials are getting importance in various applications such as hydrogen storage, fuel cell, electron field emitter etc. In order to make the cost of the gadgets utilizing carbon nanomaterials economical, efforts are being made to synthesize them at lowest possible cost. In addition, most of the processes which are being developed use precursors which are derived from petroleum products, which is destined to get depleted one day. Hence, synthesis of carbon nanomaterials based on such precursors will also get depleted and the technology based on carbon nanomaterials will come to a halt. Considering these two factors, we are making efforts to search for precursors which are plant derived and could give the desired type of products at an economical rate. Another advantage of using precursors derived from plant based materials like oil seeds, plant fibers (coconut fiber or bagasse etc) is that these materials possesses different types of morphology e.g. channel type hollow cylindrical fibers, or various types of structures having various orientation of pores etc. These varied morphologies may have some useful properties like storing of hydrogen gas, intercalating of lithium etc. Moreover, such type of structure would be extremely difficult to synthesize in laboratory. In this paper, we report the utilization of some plant based fibers and some oil seeds to make carbon nanomaterial by pyrolysing them at very high temperature in an inert atmosphere, and characterize them by SEM for their morphology. It was observed that carbon nanomaterials obtained from fibers based precursors

like coconut fiber; baggas etc have fibrous structure whereas carbon Nano materials formed from seeds of different plants show very complicated porous carbon structures. These carbon materials are being utilized for the application of Hydrogen Storage. In order to compare the utilities of plant derived carbon nanomaterials, acetylene and alcohol have also been used to prepare carbon Nano materials by the pyrolysis. However, unlike plant based precursors, these precursors needed suitable catalysts, which adds to the cost. The fibrous carbon from Bagasse (*Saccharum officinarum*) gave hydrogen adsorption of 0.656 wt% at 11kg/m² pressure of hydrogen which is nearly the same as observed with carbon nanomaterials obtained from acetylene (0.51 wt%), suggesting that plant derived precursors can be used for such purpose. Carbon nanomaterials are among the most exciting new materials to have been discovered in the past 30 years. Their remarkable properties have attracted intense interest from the scientific community, as well as from industry. With the emergence of nano science and technology, research has been initiated to exploit the unusual and unique properties of carbon nanomaterials (CNMs) that have emerged as new class of nanomaterials [1]. CNMs may exist in several forms, such as, single-walled carbon nanotubes (SWCNTs), multi-walled carbon nanotubes (MWCNTs), carbon beads, carbon fibres and nanoporous carbon. CNMs have been studied widely for potential applications in catalyst supports, optical devices, quantum computer, nanoelectronics [2], nanoelectro-mechanical systems [3] and biochips. CNMs are engineered materials targeted to exhibit unique surface morphologies; hence, they may prove to be good sorbents [4] too. Currently carbon nanofibers are used in industry for insulation and reinforcement of composites. The single and multi-walled nanotubes with diameter in the nm and length in the μm range have superior mechanical properties and have received wide attention recently. The development with nano-materials of a range of new devices in areas like electronics, photovoltaics, sensing,

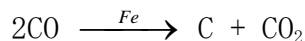
photonics and thermoelectric power is being actively pursued. However, their conduction potential has not been studied extensively. The temperature dependence of resistivity of carbon nanomaterials produced by ethanol and cotton balls is studied.

At nanometric scale the properties of the materials are different than the three-dimensional bulk forms due to difference in bond strength and short- and long-range bond order. Efforts are made to understand the correlation between the structure and properties of the materials with nanoscale diameter and with lengths varying in the micron range. The structure and properties of carbon-nanotubes (CNT) are closely related to those of graphite and related materials. The exceptional properties of CNT, an allotropic form of carbon differ from its other forms, graphite and diamond, due to the type of bonding sp^2 and sp^3 , which dominate in these materials.

CNT preparation: The chemical reactions used in CVD production of CNTs include thermal decomposition (pyrolysis) and disproportion. The easy method of the formation of CNTs is decomposition of hydrocarbon.



In the widely used method of producing nanotubes the thermal disproportionation of CO is realized on the surface of an iron/nickel/cobalt particles which acts as a catalyst:



Even before the discovery of nanotubes in 1985, carbon fibers have been prepared using the pyrolysis of hydrocarbons (CH_4 , C_2H_2 , C_6H_6 etc). So this process is widely used and is well understood. In this method the chemical

precursor along with an inert gas like Argon is allowed to pass through a quartz tube maintained at some temperature between 500 to 1300°C. Organic precursor decomposes in the form of nanotubes and are deposited on a substrate like alumina or quartz. The process yields high quality of SWNTs (single walled nanotubes) on using high purity CO as a precursor at the temperature between 900 and 1300°C. A schematic diagram of the catalytic chemical vapour deposition (CVD) is given in Fig. 1

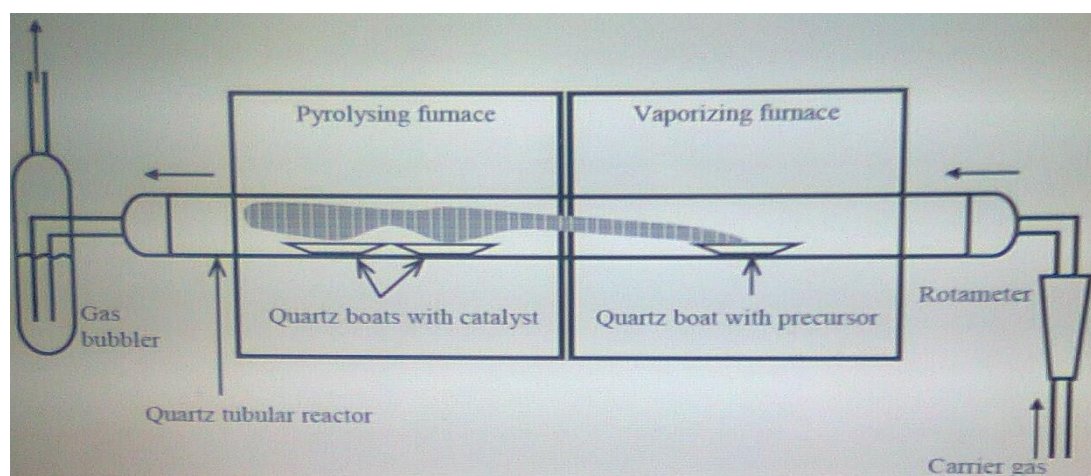


Fig. (1) A schematic diagram of CVD set up

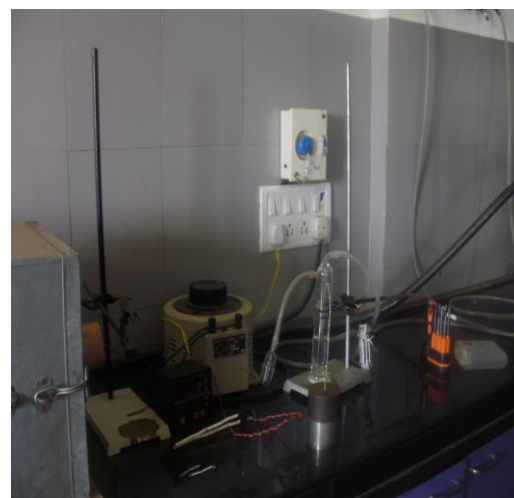


Fig2 The experimental set up of the CVD process

Chemical vapour deposition of hydrocarbons over a metal catalyst is a classical method that has been used to produce various carbon nanomaterials such as carbon fibers and filaments for over twenty years. Recently large amounts of CNTs are also formed by catalytic CVD of naturally occurring substances like tin oil, pine oil, mustered oil, camphor etc over Nickel, Cobalt and Iron catalysts supported on silica. Precursors which are plant derived are used mainly for the low cost production and to get various types of structures of carbon nanomaterials. The carbon deposition activity seems to relate to the cobalt content of the catalyst, whereas the CNTs selectivity seems to be a function of the pH in catalyst preparation. Fullerenes and bundles of single walled nanotubes were also found among the multi walled nanotubes produced on the carbon catalyst. These can be grown as individual wires or as an ensemble to build functional devices.

We have prepared CNTs by both ways (i) using hydrocarbons and (ii) using cotton (plant derived precursor).

Experimental procedure:

CNT preparation involves the following steps: (a) Catalyst preparation (b) CNT deposition on catalyst (c) Purification of CNT.

Catalyst preparation: Nitrates salts of Ni, Co or Fe were chosen so that we can get metal catalyst easily as oxides of nitrogen will escape leaving behind metal oxide. Known weight of nitrate salt of respective metal with urea in an appropriate ratio (1:3) is mixed and grounded uniformly. It is converted into liquid while grinding after some time. It is then heated in a crucible over a burner. A muffle furnace having temperature 600°C can also be used to prepare metal oxides from the nitrate salts. After heating it is grounded to get the oxide of the catalyst in powder form. The percent yield is calculated.



Fig3 Nickel oxide obtained from Nickel nitrate

Reduction of metal oxide into metal catalyst:

The reduction of metal oxide was performed in the laboratory by using a CVD unit consisting of two furnaces joined side by side with a quartz tube traversing both of them (Fig. 1a). Detailed catalyst preparation, synthesis and treatment methods have been described above [5,6]. Pyrolysis of organic

precursors at high temperature facilitated by catalyst leads to CNM formation. In the CVD process, 10ml of ethanol was filled in a quartz boat and kept in the vaporizing furnace. Two quartz boats each containing 0.5 g of catalyst was kept in the pyrolysing furnace. After inserting the quartz boats within the quartz tube, one end was connected to the carrier gas inlet and the other end was connected to the gas bubbler through which the gas was vented. Initially, carrier gas flow was initiated (50 mL/min) to ensure an oxygen-free environment inside the quartz tube. The pyrolysing furnace set at a predetermined temperature 600°C was switched on after 15 min. The vaporising furnace also set at the desired temperature was switched on after the temperature of the pyrolysing furnace was stabilized. As the ethanol started vaporizing, dark brown fumes were observed to emerge through the gas bubbler. After 10 min, the dark brown vapour was no longer observed, thus indicating complete vaporization of ethanol. Both furnaces were then switched off and allowed to cool. Throughout the process, the carrier gas flow rate was maintained constant. After cooling of the furnace, the catalyst boats and precursor boat were taken out. The carbon deposited on each boat was weighed and stored for further purification.



Fig4 The deposition of Carbon nanoparticles on Ni- catalyst in a quartz plate



*Fig5 The deposition of Carbon nanoparticles on Fe- catalyst
in a quartz plate*



Fig6 The deposition of Carbon nanoparticles on Co -catalyst in a quartz plate

For hydrogenation process we used the split furnace since we can perform CNT deposition also in the same furnace. For hydrogenation the catalyst is kept in zone-1 having temperature 650° C for an hour. Hydrogen gas is passed through the furnace to convert metal oxide into pure metal. So we get pure metal in zone-1.

Deposition of CNT takes place in the same furnace with some changes in its settings. Argon gas is now passed through the furnace to make the atmosphere inert at temperature 650° C. Argon gas is passed for 1 hr since deposition takes place for approximately for 1 hr. In zone -2 the precursor ethanol/cotton is kept. The temperature of this zone is lower than that of zone-1. The vaporised oil (CNT) deposits on the metal catalyst. After

completion of deposition the furnace was allowed to cool. Carbon nanotubes were collected and weighed.

Purification of CNT:

Suspension of the whole amount of CNT in hydrochloric acid is made. It is stirred well and kept overnight. It is then filtered with the help of What-man filter paper and kept in muffle furnace for drying at about 50-60° C for at least 30 min. Percentage yield is calculated.

Surface area measurement:

The average surface area of the particle is determined by using the BET in liquid phase by carbon nanotubes.

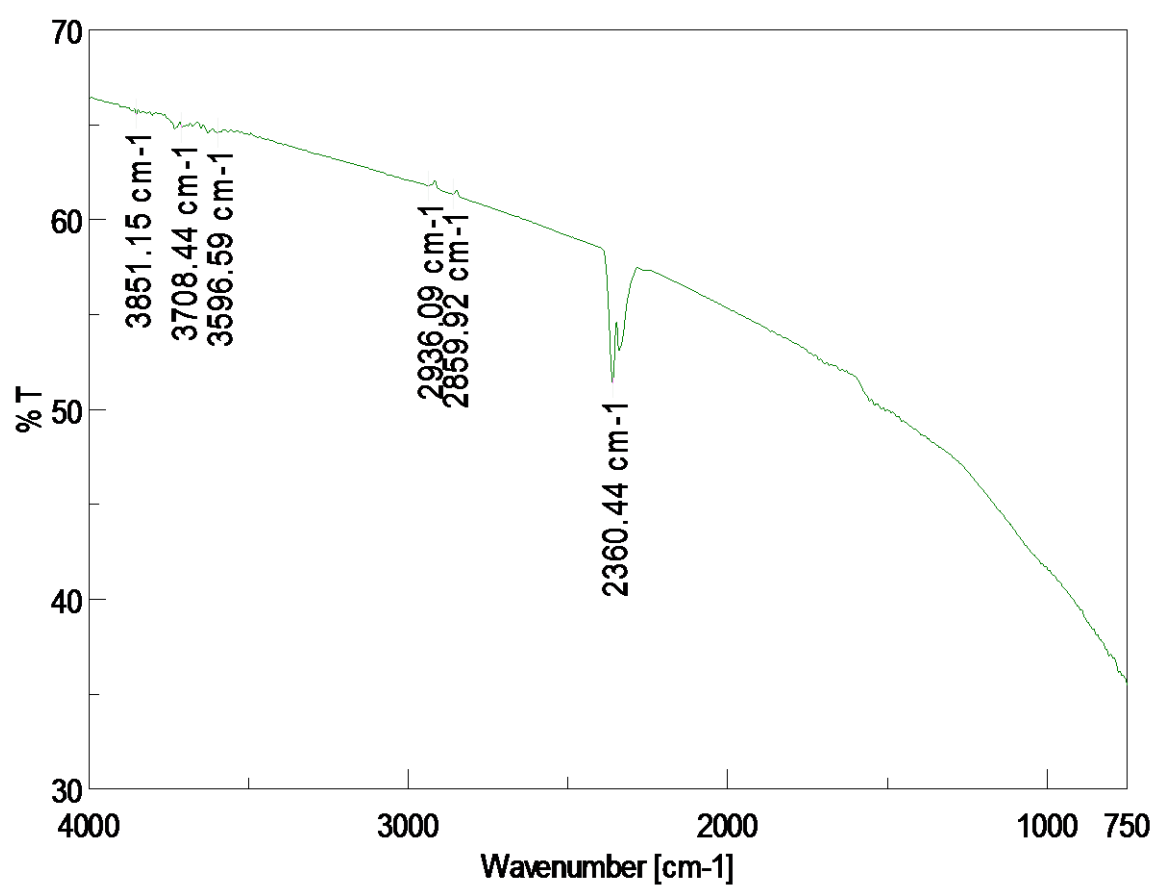
Characterization:

The measured average surface area of carbon nanomaterials obtained in the CVD process confirms the formation of carbon nanoparticles ranging from few nm to μm in size.

FTIR: The FTIR data shows the formation of carbon nanoparticles

The FTIR of the samples confirm the formation of Carbon nanomaterials.

It is found that the resistivity ρ (T) decreases with temperature. It is generally agreed that single walled carbon nanotubes at room temperature are good conductors with large mean free path and the resistivity changes from non-metallic to weakly metallic at $T \sim 200\text{K}$. The high resistivity at low temperature is attributed to the strong localization of charge carriers.



Resistivity:

The data shows decrease in resistivity with temperature.

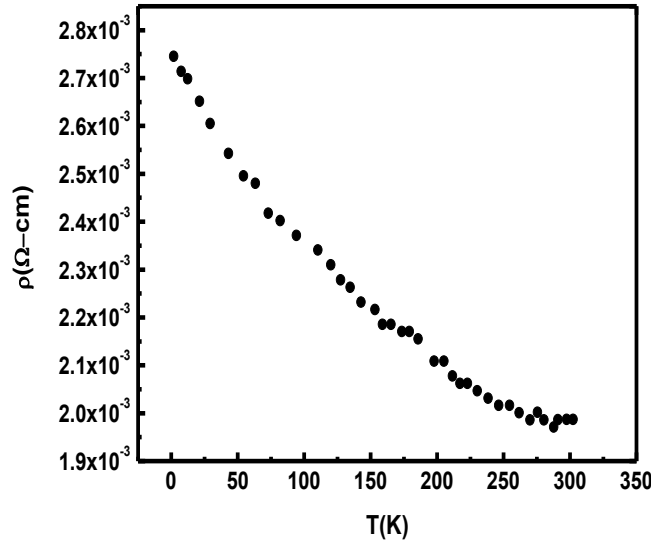


Fig.7(a) &7(b). Resistivity vs temperature curve is plotted for CNT prepared by til oil. In both the curves the semiconducting nature of CNT is seen. Near room temperature it obeys Mott's theory. At low temperature the high resistivity can be due to localization of charges.

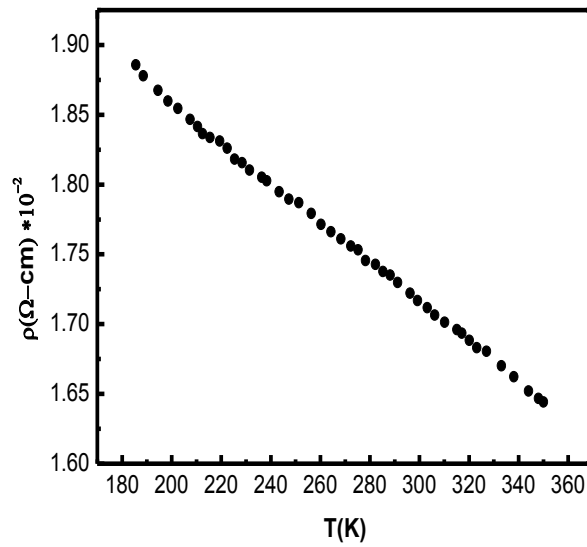


Fig. 7(b)



Fig8 The four probe device to measure resistivity of CNTs

Electrical transport in CNTs and fiber: small polaron conduction

We account for the residual resistivity and the metal-insulator transition observed in SWNT fibers on the basis of the correlated polaron model. In this electrons with two neighbouring carbon atoms exchange their orbital states through phonon coupling to the zero-point vibrations and thermal phonons thereby forming the small polaron state that moves from one site to another through quantum tunneling. The electrical transport in single-wall carbon nanotubes (SWNT) has been shown to follow the characteristics of conducting wires [9,10]. Electronic devices can be constructed from the fiber forms which retain the excellent axial properties expected from

infinitely long tubes. A cost-effective method of production of such fibers comprises of the injection of a SWNT suspension through an orifice into a co-flowing stream of an aqueous solution that contains a polymer such as polyvinyl alcohol (PVA) as a coagulating agent [11,12]. These fibers have high strength, light weight and thermally and electrically conducting structural elements and can be used for the construction of electronic devices. The difficulty in their use is that the mechanical, electrical and thermal properties depend on the SWNT alignment and the presence of the insulating PVA in the fibers [13]. It is found that room temperature resistivity decreases by more than a factor of 3 as the nanotube alignment is improved and the resistivity decreases by almost four orders of magnitude when PVA is removed through thermal annealing [14]. The general features of the $\rho(T)$ curve with and without PVA are almost the same despite the difference of four orders of magnitude in the resistivity except that for the composite fiber $\rho(T)_{T \rightarrow 0}$ diverges more strongly than the annealed one without PVA. This has led to the suggestion that the transport mechanism in the fiber in the two cases, with and without polymer, should be different [14]

It is generally agreed that pure SWNTs at room temperature are good conductors with very large mean free path [15] and the resistivity changes from nonmetallic to weakly metallic at $T \sim 200$ K. The increase in $\rho(T)$ at low T arises from the strong localization of carriers [16] In interpreting the results of the temperature dependence of the resistivity of the pure SWNT fibers Badaire et al [14] find good fit to the Mott-type phonon-assisted variable range hopping (VRH) at low temperature, $T < 25$ K, but with unphysical parameters.

Roche et al [17] have recently reviewed the role of electron-phonon coupling in quantum transport of the carbon nanotube. In

this letter we limit our discussion to only dc electron conductivity in long SWNT fibers and explore the mechanism of transport. We consider only the low-bias regime for which the propagating electron couples to low energy phonon mode [18] and the SWNTs behave as ballistic conductors owing to the reduced back scattering from elastic disorders like vacancies, topological disorders etc [19]. For this case Roche et al [17] find the electron-phonon coupling mainly comes from the twisting (TW) mode for which the mean free path is longer than $1\mu\text{m}$ and scattering has diffusive characteristics, $l_{\text{TW}} \propto 1/T$. Fisher [20] has tried to calculate the experimental resistivity of a SWNT fiber of length L at 300K assuming that each metallic tube is a perfectly aligned sample of finite length ballistic conductors in series, the length L of the metallic tube being treated as the elastic mean free path for the electron-phonon back scattering. Then $\rho = (\text{area/tube}) / (2G_0L)$ where the conductance quantum $G_0 = 2e^2 / h = (12.6 \text{ K}\Omega)^{-1}$. Taking the radius of the tube as 1.5 nm and $L = 300 \text{ nm}$, $\rho = 15 \mu\Omega\text{-cm}$.

We adopt a slightly different approach to obtain the expression for resistivity. The quantization condition is determined by the wrapping of the grapheme sheet. We consider that the electron hops from one end of the diameter d_t to the other with the momentum $k = \pi / d_t$ in the metallic state. The lower limit for the mobility is defined by the uncertainty relationship, $\tau_s \sim \hbar/W$, where the bandwidth $W = \hbar^2 k^2 / 2m^* = (\hbar^2/2m^*)(\pi / d_t)^2$. Here m^* is the effective mass of the electron that is confined within the tube. The mobility is $\mu = e \tau_s / m^* = 2ed_t^2 / \pi^2 \hbar$. To estimate n in $\rho = (ne\mu)^{-1}$ we take two atoms per hexagon of the graphene sheet with area $3\sqrt{3}a^2/2$ where a is the carbon-carbon bond length, 1.42\AA . There is one electron per atom, then the upper limit of the electron density is

$$n_{\max} = \frac{16}{(3\sqrt{3} d_t a^2)} \quad \dots\dots\dots (1)$$

For this we obtain

$$\rho = \frac{(3\sqrt{3} / 16) (\pi a^2 / 2G_0 d_t)}{\dots\dots\dots} \quad (2)$$

With $d_t \sim 3\text{nm}$, $n_{\max} = 5 \times 10^{28} / \text{m}^3$ and $\rho \sim 5 \mu \Omega\text{-cm}$. For the stochastic tube growth with respect to the wrapping only 1/3 of the tubes are metallic, so $\rho \sim 15 \mu \Omega\text{-cm}$, nearly the same as the value of graphite. Note in this approximation the resistivity depends only on the diameter of the tube. This estimate agrees within an order of magnitude with the observed resistivity of pure SWNT fibers at 300 K $\sim 200 \mu \Omega\text{-cm}$ [13]. As remarked by Fischer [20] this is a surprising result as there are many factors that will increase ρ in real samples, like the distribution in d_t , unaligned tubes, vacancies, distribution in the length L of the tubes, junction resistance between tube junctions, elastic scattering from tube ends, defects and impurities. Further, the resistivity shows non-metallic behaviour at low T and levels off to a residual resistivity, $\rho(0)$, and does not diverge as $T \rightarrow 0$. There is a metal to insulator (MI) like transition near $T \sim 200 \text{ K}$ as above this temperature the resistivity linearly increases with temperature though very slowly. These two striking features, absence of the usual scattering processes found in the 3D metals and presence of the MI transition, indicate the quantum nature of transport in the nanotubes..

Srivastava has proposed [21, 22] a correlated polaron model where electron itineracy is promoted by valence exchange in mixed ionic compounds like

manganites $\text{La}_{1-x}\text{A}_x\text{MnO}_3$ (A = Ca, Sr...), ferrites and high T_c oxide superconductors. In a system with an anion or cation in a mixed valence state on the crystallographic equivalent sites there are always two possible ways to arrange the ions that can be represented by two degenerate states, Ψ_1 and Ψ_2 . The degeneracy is removed on coupling to a phonon mode and forming a small polaron state. The polaron shift energy ε_p plays a dominant role in the transport [21,22]. The dc conductivity is given by the Josephson weak link like current-phase relationship ($k_B = 1$, $\beta = 1/T$),

$$\sigma = \frac{1}{4} [n e^2 a^2 \omega_0 \text{sech}^2(\varepsilon_p \beta / 2)] \quad \text{-----} \quad (3)$$

Here n is the electron density, a is the jump distance and ω_0 is the phonon frequency.

A similar situation arises in the nanotubes. In the hexagonal graphite lattice the two neighbouring sites A and B can be occupied by two distinct types of electron orbital states $\phi(x)$ and $\chi(x)$, separated by a small energy difference δ [23]. $\phi(x)$ may arise from the π molecular orbital and $\chi(x)$ from π^* as the two bands are degenerate at the Fermi energy in metallic nanotubes. In that case there may be equal negative charge associated with the two nuclei but there can exist a homopolar dipole due to unequal charge distribution [24]. With appropriate coupling with a specific phonon mode the degenerate states Ψ_1 and Ψ_2 may form a vibronic state with lower energy as in the mixed valence state. The superlattice states

$$\psi_1 = \sum_{i \in 2..} e^{i k r} \phi_i + \sum_{i \in 1,3..} e^{i k r} \chi_i \quad \text{and}$$

$$\psi_2 = \sum_{i \in 2..} e^{i k r} \chi_i + \sum_{i \in 1,3..} e^{i k r} \phi_i$$

are degenerate. ψ_1 and ψ_2 for $k = 0$ can be coupled via the phonon energy ω_0

as these can be expressed as ($\hbar = 1$) [21]

$$\psi_1 = \frac{1}{\sqrt{2}} (e^{ikx} + e^{-ikx}) \text{ and } \psi_2 = \frac{1}{\sqrt{2}} (e^{ikx} - e^{-ikx})$$

$$\psi_1' = \frac{1}{\sqrt{2}} (ik e^{ikx} - ik e^{-ikx})$$

$$\psi_2' = \frac{1}{\sqrt{2}} (ik e^{ikx} + ik e^{-ikx})$$

where the prime denotes the time derivative. Eq(3) is then obtained for

$$\rho = \frac{1}{n_1 n_2} \left(\frac{1}{\psi_1'} \frac{d\psi_1}{dt} + \frac{1}{\psi_2'} \frac{d\psi_2}{dt} \right)$$

and $n_1 = n_2 = n$.

It is possible to obtain Eq(3) also from the Holstein Hamiltonian for the small polaron [22]. This is similar to the Hamiltonian description of the charge transport in the carbon nanotubes [17] At low temperature ($T < \theta_D/4$) the zero-point vibrations dominate over the thermal phonon process that lead to Eq(3) [25]. Here θ_D is the Debye temperature. Including the contribution from zero-point vibration the resistivity is expressed as

$$\rho(T) = A (\theta_D/4 + T) \cosh^2(\epsilon_p/2(T + \theta_D/4)) \quad \text{-----} \quad (4)$$

where from Ref [24]

$$A = 1.13 k_B / d_t^2 e^2 \nu_{ph} n \quad \text{-----} \quad (5)$$

Here ν_{ph} is the phonon frequency. Eq (4) gives the residual resistivity,

$$\rho(0) = (A \theta_D/4) \cosh^2(2 \epsilon_p / \theta_D) \quad \text{-----} \quad (6)$$

There is a metal to insulator transition at T_{MI} for

$$\partial \rho / \partial x = 0 \text{ with } x = T + \theta_D/4,$$

$$T_{MI}=0.85 \varepsilon_p - 0.25 \theta_D$$

$$----- (7)$$

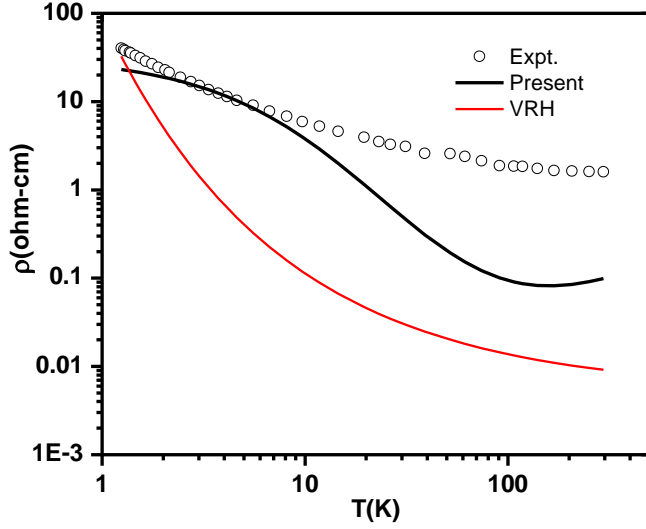


Fig.9 Resistivity vs temperature curve for annealed (76% stretch) SWNT fiber. The experimental curve is from Ref. [14]. The curve in black is from Eq(4) with $A = 2.5 \times 10^{-4} \Omega\text{-cm-K}^{-1}$, $\varepsilon_p = 293 \text{ K}$ and $\theta_D = 120 \text{ K}$. The curve in red is from Mott's VRH model with $\rho_M(0) = 7.7 \times 10^{-3} \Omega\text{-cm}$ and $T_0 = 95$ from Ref. [22]

In Fig 9 the $\rho(T)$ curve for an annealed (76 % stretch) SWNT fiber from Ref [14] in the log-log scale is given. Also given is the curve in red for $\rho(T) = \rho_M(0) \exp[T_0/T]^{1/2}$ obtained on Mott's phonon-assisted variable range hopping model (VRH) with the characteristic temperature $T_0 = 95 \text{ K}$ [14]. For the present analysis $\rho(0)$ in Eq. (6) is taken as $\rho(1.5 \text{ K}) = 22 \Omega\text{-cm}$. For this value $\rho_M(0) = 7.7 \times 10^{-3} \Omega\text{-cm}$. The plot from Eq(4) is given in black with $A = 2.5 \times 10^{-4} \Omega\text{-cm-K}^{-1}$, $\varepsilon_p = 293 \text{ K}$ and $\theta_D = 120 \text{ K}$. From Eq. (7) $T_{MI} = 219 \text{ K}$. The smallest frequency of the phonon mode in SWNT

is that of the radial breathing mode with $\nu_{ph} = 187.1 \text{ cm}^{-1}$ [17]. Taking this value and $d_t = 3\text{nm}$ from Eq. (5) $n \sim 5 \times 10^{25}./\text{m}^3$ This is not unreasonable.

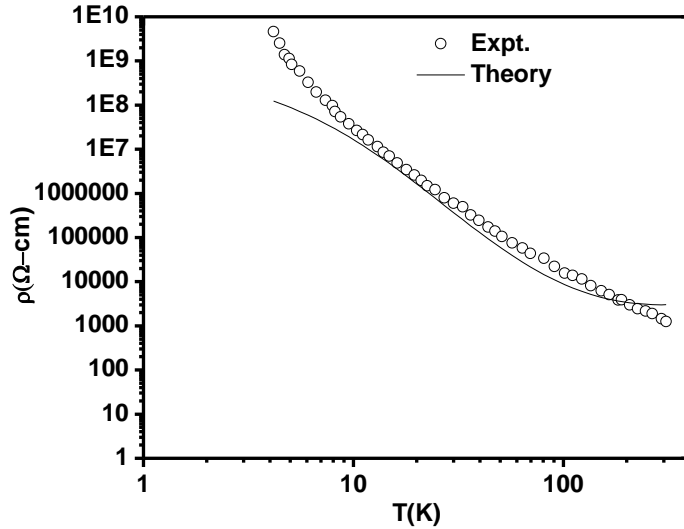


Fig.10 Resistivity vs. temperature curve for the composite 53% stretch fiber. The experimental curve is from Ref.[14]. The theoretical curve is from Eq.(4) with $A = 1.77 \text{ } \Omega\text{-cm-K}^{-1}$ $\epsilon p = 506 \text{ K}$ and $\theta_D = 120 \text{ K}$

In Fig. (2) the $\rho(T)$ curve for the composite 53% stretch fiber from Ref. [14] is given and compared with the theoretical curve from Eq. (4) with $A = 1.77 \text{ } \Omega\text{-cm-K}^{-1}$, $\epsilon p = 506 \text{ K}$ and $\theta_D = 120 \text{ K}$. From Eq. (7) T_{MI} is 400 K. The agreement is good for $10 < T < 300 \text{ K}$.

The orbital exchange model presented here reproduces the main features of dc transport in SWNT fibers, the weak temperature dependence in the metallic region, $\rho \propto T$ for $T > T_{MI}$ and non-metallic behaviour for $T < T_{MI}$ with a non-diverging $\rho(T)_{T \rightarrow 0}$ and a well defined residual resistivity, $\rho(0)$ for pure fibers. Because of this Mott's variable range hopping model does not agree well with the experiment (Fig.1). The variation of resistivity with temperature for samples with different stretch ratio for PVA composite

nanotubes can also be explained by the correlated polaron model and another mechanism of transport with and without the polymer as suggested in Ref. [14] is not required.

Conclusion:

It is generally agreed that single walled carbon nanotubes at room temperature are good conductors with large mean free path and the resistivity changes from non-metallic to weakly metallic at $T \sim 200\text{K}$. The high resistivity at low temperature is attributed to the strong localization of charge carriers. Carbon nanomaterials have many properties- from their unique dimension to an unusual current conduction mechanism that make them ideal components of electrical circuits. They offer an outstanding playground to challenge the quantum theory at the nanoscale, manifesting novel physical phenomenon. Amongst various properties electronic transport stands as a driving force to scientific excitement and technological innovation in CNTs. The charge carrier transport in carbon nanotubes, though a complex phenomenon but probably could be explained through electron-phonon coupling. In future, work can be done to increase the conductivity of CNT by treating it with acids like HNO_3 .

Other potential application of carbon nanomaterials:

Carbon nanotubes (CNTs) have shown exceptional adsorption capability and high adsorption efficiency for various organic pollutants such as benzene [14], 1,2-dichlorobenzene [15], trihalomethanes [16] and polycyclic aromatic hydrocarbons (PAHs) [17]. CNTs were found to be superior sorbents for inorganic pollutants such as fluoride [18], and several divalent metal ions [7,8,19-25]. Li et al. [24] reported that CNTs with more defects and poor quality possess higher surface area and exhibit better lead sorption capacity compared to aligned CNTs. Activation of CNTs plays an important role in enhancing the maximum sorption capacity. Activation causes modification in the surface morphology and surface functional groups and causes removal of amorphous carbon. Activation of CNTs under oxidizing conditions with chemicals such as HNO_3 , KMnO_4 , H_2O_2 , NaOCl , H_2SO_4 , KOH , and NaOH have been widely reported [8,21,26]. During activation, the metallic impurities and catalyst support materials are dissolved and the surface characteristics are altered due to the introduction of new functional groups [24,26]. Both Langmuir and Freundlich adsorption models have been used for representing sorption.

References:

- [1] G. Dresselhaus, M.S. Dresselhaus and P. Avouris, Carbon Nanotubes Synthesis, Structure, Properties and Applications. Springer, Berlin, 2001.
- [2] A.K. Chatterjee, M. Sharon and R. Banerjee, J. Power Sources, 117(1-2) (2003) 39-44.
- [3] J. W. Kang and H. J. Hwang, J. Comput. Theor. Nanosci. **6**, 2347 (2009)
- [4] G. Dresselhaus, M.S. Dresselhaus and P. Avouris, Carbon Nanotubes Synthesis, Structure, Properties and Applications. Springer, Berlin, 2001.
- [5] A.K. Chatterjee, M. Sharon, R. Banerjee and M. Neumann-Spallart, Electrochim. Acta, 48(23), (2003) 3439-3446.
- [6] A.K. Chatterjee, M. Sharon and R. Banerjee, J. Power Sources, 117(1-2) (2003) 39-44.
- [7] J. Kong. Et al. , Appl. Phys. A **69** 305 (1999)
- [8] M S Fuhrer et al., Solid state Commun. **109** , 105 (1998)
- [9] S. J. Tans et al. , Nature (London) 386 474 (1997)
- [10] M. Backrath et al. , Science **275** 1922 (1997)
- [11] B. Vigolo et al. , Science **290** 1331 (2000)
- [12] P. Poulin, B. Vigolo, and P. Lannois, Carbon **40** 1741 (2002)
- [13] W. Zhou et al. , J. Appl. Phys. **95** 649 (2004)
- [14] S. Badaire et al. , J. Appl. Phys. **96** 7509 (2004)
- [15] J. Kong. Et al. , Appl. Phys. A **69** 305 (1999)
- [16] M S Fuhrer et al. , Solid state Commun. **109** , 105 (1998)
- [17] S. Roche et al., J. Phys. Condens. Matter **19** (2007) 18 3203
- [18] G. Penninglin and N. Goldsman Phys. Rev. B (2003) 68045426
- [19] P. L. McEuen et al. , Phys. Rev. Lett. **83** (1999) 5098

- [20] J. E. Fischer in ‘Nanotubes and Nanofibers’ Ed. Y Gogotsi , Tayer & Francis (2006) p20.
- [21] G.Srinivasan and C.M.Srivastava, Physica Status Solidi b **103** 665(1981)
The valence exchange and the correlated polaron model in mixed-valence compound Fe_3O_4 was first introduced in this paper. It is used by G. Glitzer and J. B. Goodenough ‘Mixed - Valence iron oxides’ in ‘Structure and Bonding’ **61** , 1 (1985) and for manganites and high T_c superconductors by C. M. Srivastava, Jour. Mag. Soc. (Japan) **22**, Supp.S1, 15 (1998).
- [22] C .M. Srivastava, Pramana, Jour.Phys. **50** 11 (1998), J. Phys. Condens. Matter **11** 4539 (1999)
- [23] G. W. Semenoff et al., Phys Rev.Lett. **53** 2449 (1984)
- [24] C.A.Coulson, “Valence” (Clarendon Press, Oxford, 1952)p.145
- [25] Saket Asthana et al Physica B **371** 241 (2006) In this paper $\bar{\theta}_D$ has been used as the limit of applicability of the zero-point vibrations. Here we have taken θ_D as a fitting parameter.
- [26] S.V.Rotkin and S. Subramoney, Applied Physics of Carbon Nanotubes: Fundamentals of Theory, Optics, and Transport Devices (Springer-Verlag-Berlin, Heidelberg, 2005)

UGC

Minor Research Project Report

Submitted by

Dr. Neeta B Srivastava

Dept of Physics

**Ramniranjan Jhunjhunwala College, Ghatkopar
Mumbai**

2012 - 2014

Acknowledgement

I express my deep sense of gratitude to my principal Dr. Usha Mukundan for her valuable guidance, motivation and full attention at all stages in my project work and for providing me infrastructure without which it was impossible to complete my project.

I sincerely thank our H.O.D. Prof. Raghu Pillai for giving me permission to carry out our research work anytime, without which I hardly can complete my project work.

I would like to thank Prof. Mahesh Sharon and Dr. Madhuri Sharon with immense pleasure for their valuable guidance and constant encouragements which I have received during my experimental work.

Neeta B Srivastava